IEEE Access
Multidisciplinary ⋮ Rapid Review ⋮ Open Access Journal

Received February 8, 2022, accepted March 5, 2022, date of publication March 8, 2022, date of current version March 24, 2022.

Digital Object Identifier 10.1109/ACCESS.2022.3157982

A Unified Active Damping for Grid and Converter Current Feedback in Active Front End Converters

EDI MATIJEVIC[1], (Member, IEEE), RAHUL SHARMA[1], (Senior Member, IEEE), FIRUZ ZARE[2], (Fellow, IEEE), AND DINESH KUMAR[3], (Senior Member, IEEE)

[1]School of Information Technology and Electrical Engineering, The University of Queensland, Brisbane, QLD 4067, Australia
[2]School of Electrical Engineering and Robotics, Queensland University of Technology, Brisbane, QLD 4000, Australia
[3]Global Research and Development Center, Danfoss Drives A/S, 6300 Grasten, Denmark

Corresponding author: Edi Matijevic (e.matijevic@uq.edu.au)

This work was supported by the Australian Research Council under Project FT150100042 and Project LP170100902.

ABSTRACT The Active Front End (AFE) is interconnected to the grid with an LCL filter to reduce the switching harmonics. Possible resonances induced by the LCL filter can be damped using Active Damping (AD). In AFE applications, the current sensor can be placed on either the grid-side or the converter-side, resulting in different frequency responses. This paper presents a novel active damping approach that is universally applicable to all active front end converters regardless of whether the current sensor is placed on the grid side or the converter side. At the heart of the proposed approach is a practically implementable fourth-order filter that dampens the resonance whilst being capable of mitigating the challenges associated with both grid current feedback and converter current feedback. These include amplifications associated with derivatives in active damping term with grid current feedback and high susceptibility to instability with converter current feedback due to digital delay. The proposed active damping is thoroughly investigated in terms of practical implementation issues such as different LCL filter parameters, different sampling methods, grid impedance, and digital delay. The approach is experimentally validated on motor drives consisting of 2 two-level three-phase converters interfaced with a dSPACE rapid control prototyping system across a wide range of resonant frequencies and PWM sampling methods. Stability analysis is performed on both current control methods to validate that active damping assures stable operation for a wide range of resonant frequencies and grid impedance.

INDEX TERMS Active front end converter, active damping, digital delay, discrete system, stability analysis, resonance damping, current control, LCL filter.

I. INTRODUCTION

In recent years, power electronics technology development has had a significant impact on renewable energy [1] and the motor drive industry, however, with the penetration of non-linear elements, new problems are emerging. Mainly, the growth of non-linear loads has a magnifying effect on the current distortion [2] and voltage waveforms (THD), consequently, polluting the grid [3], [4]. Therefore, one of the main goals for researchers is to reduce THD injected into the grid [5].

The industrial motor drives [6] even though not as attractive topics as renewable energy [7] and electric vehicle [8], have a critical role in global industries and world suitability. A typical industrial motor drive consists of a front-end rectifier (either passive or active) connected to the grid, 2-level voltage source inverter supplying a three-phase current to the motor, and a controller associated with it as shown in Figure 1. Desirably, if an active front-end converter is used as a front end of the drives, then THD requirements can be fulfilled due

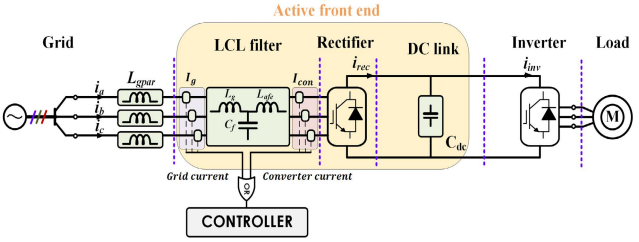

FIGURE 1. Industrial motor drives based on AFE topology.

The associate editor coordinating the review of this manuscript and approving it for publication was Jiefeng Hu.

to AFE's capability to draw sinusoidal currents. As an active front-end converter operates as a PWM converter, L or LCL filters are required to provide attenuation for high switching frequency. The combination of PWM converter and low pass filter produces an advantageous alternative to diode rectifiers, which in regards to diode rectifier improve THD drastically. The objective of AFE is to control the DC-link capacitor voltage as per a set reference value independent of connected load while also controlling grid current to a reasonable THD, thereby delivering THD improvements relative to the diode bridge used in the past. The use of active switches such as IGBTs rather than diodes are the main difference between AFE and diode bridge rectifiers. In addition to the ability to draw sinusoidal currents, the active solution provides controllable DC-link voltage, bidirectional power flow, and unity power factor.

The most common type of filter used in combination with AFE is the LCL filter due to the inherent -60 dB/dec attenuation property. However, the LCL filter introduces resonance which has to be properly damped by either passive [9], active [10] or hybrid damping [11]. Active damping can provide advantages over passive damping in terms of efficiency at the cost of additional sensors and implementation complexity. Generally, passive damping is implemented by adding a resistor in series with a filter capacitor, however, the resistor will add extra zero into the transfer function, inherently reducing LCL filter attenuation to $-40\,dB/Decade$ after resonant frequency. This is undesirable due to the high switching frequency of PWM, which requires filtering. Aside from simple passive damping techniques that use a resistor in series or parallel with the LCL filter components [12], there are also more complex other options, such as a split capacitor with series resistor [13], which optimizes power loss and size, but is parameter-sensitive and inherently amplifies switching harmonics, thus, active damping is necessary for many applications.

Many active damping solutions focus on additional capacitor current [14] or voltage sensors [15] to implement active damping due to simplicity. However, the current control objective can be used as a feedback method for active damping, removing additional sensors that are required in conventional active damping techniques [16].

Recent advances in current controller research suggest that controls such as multi-frequency current controllers [17] and model predictive controllers [18] do not suffer from the same stability issues as traditional PI or PR in different frames due to resonance and active damping is not necessary. However, the drawback of recent controls is the high computational burden. Conventional control as voltage-oriented control, on the other hand, remains popular and widely used in industry due to its simplicity and lower computational cost.

Mainly, two different types of current feedback are used for AFE voltage-oriented control. In industry, converter current feedback is usually implemented due to easier execution of circuit protection, while grid current can generally provide better performance. Considering that the resonance is the dominant frequency in frequency response for both control techniques, it is feasible to design active damping capable of damping resonance for both control mechanisms. Thus, a reduction in the number of sensors while not sacrificing system performance is a control objective for any practical motor drive system. In a desire to reduce the number of sensors, this paper considers AFE universal active damping method for both converter and grid current feedback control methods.

This paper is an extension of the previous paper presented in [19]. This comprehensive active damping proposal contains a number of important novelties. The main difference and additional novelty is the inclusion of the converter side control active damping and the unification of the active damping method to fit both control techniques. There is no research that the authors are aware of that proposes a unified damping approach for the two main feedback methods used in voltage-oriented control AFE. The discrete investigation of stability, which shows proposed active damping robust behavior under various LCL filter parameters, is also a key novelty. Grid impedance and various sampling methods have also been investigated, demonstrating the versatility of proposed active damping under various conditions. The proposed active damping is implemented and validated in experiments conducted by stabilizing unstable systems and evaluating their response under transients. A summary of the novelties presented in this paper is as follows:

- A unique unified active damping approach for both grid and converter side current feedback independent on LCL filter resonant frequency and sampling method
- Discrete domain analysis of the proposed active damping under a diverse selection of LCL filter parameters.
- In-depth stability analysis taking into account various grid impedances and resonant frequencies.
- Experimental validation on motor drive consisting of 2 two-level three phase converters interfaced with a dSPACE rapid control prototyping system.

The paper is organized as follows. Section II analytically describes the system of interest. Section III introduces proposed active damping control. Stability analysis is investigated in section IV while section V provides simulation and experimental results of the proposed control. Finally, the conclusion is presented in section VI.

II. SYSTEM DESCRIPTION

The system diagram is shown in Figure 1. A conventional three-phase two-level voltage source converter is interfaced to the grid through an LCL filter. Either grid or converter current measurements are needed for the implementation of the control. If properly designed, the AFE converter provides stable low ripple DC-link voltage, low grid current THD, and close to unity power factor.

A. CONVERTER AND GRID SIDE CURRENT CONTROL

The advantage of LCL filters over conventional L filters is that they offer much better harmonic attenuation

characteristics for the smaller footprint. Therefore, to improve current harmonic attenuation and economical cost, the LCL filters are increasingly used when connecting voltage source converters to the grid.

Considering both control feedback and LCL filter, open-loop transfer functions are derived where equation (1) relates to grid current control while (2) relates to converter side control. AFE LCL filter per phase is derived from the block diagram in Figure 2 as an output control objective grid current I_g or converter current I_{con} and input PWM voltage U_{afe}.

$$G_g(s) = \frac{I_g}{U_{afe}} = \frac{1}{L_{afe}L_gC_fs^3 + s(L_g + L_{afe})} \tag{1}$$

$$G_c(s) = \frac{I_{con}}{U_{afe}} = \frac{1 + C_fL_gs^2}{L_{afe}L_gC_fs^3 + s(L_g + L_{afe})} \tag{2}$$

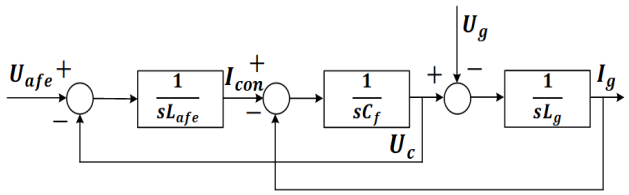

FIGURE 2. Block diagram of the LCL filter.

Aside from the two control methods, depending on the single or double update PWM sampling method used, delay can inherently change the system frequency response.

Assuming no resistance is included in series with filter components, LCL-filter introduces resonance in both of the control types shown in Figure 3 a) that has to be properly damped to ensure system stability. Two main differences seen from bode plots in the figure are converter side anti-resonance introduced by second-order zero, and reduced attenuation to $-40dB/dec$ after resonant frequency poles. However, apart from the frequency response differences, both controls have different inherent stability. Grid side current control (G_g) is inherently unstable while converter side current control (G_c) is stable considering ideal characteristics. However, taking into consideration the digital delay introduced by sampling and PWM, additional phase lag is added to the system that causes phase margin to decrease, making the converter control system unstable as seen in Figure 3 b).

Grid side current control, on the other hand, can become stable in some resonant frequency regions with enough delay without the need for active damping [20]. However, as controllers become faster, delays decrease, necessitating the use of active damping.

Table 1 summarises the effect of delays on stability for various control methods, where:

$$10\,f_{line} < Low\,f_{res} < f_{critical} < High\,f_{res} < \frac{f_{sw}}{2} \tag{3}$$

where $f_{critical}$ is defined as $\frac{f_{res}}{f_{samp}}$. The frequency between 10 f_{line} and critical frequency is defined as $Low\ f_{res}$ while $High\ f_{res}$ is a frequency between critical frequency and half

TABLE 1. Stability under influence of delays.

Control methods	Stability	
	Low ω_{res}	
	Single update	Double update
Converter side	Stable	Stable
Grid side	Unstable	Unstable
	High ω_{res}	
	Single update	Double update
Converter side	Unstable	Unstable
Grid side	Stable	Stable

of the switching frequency. Critical frequency compared to investigated switching frequency (10 kHz) is 0.167 as a ratio $\frac{f_{res}}{f_{samp}}$ or in terms of frequency (3.34 kHz) for double update, and 1.67 kHz for single update similarly as in [20]. Critical frequency is the threshold frequency where each control method passes the stability criterion shown in Table 1. Considering that delays will be different depending on if the PWM sampling is single or double update [21], they affect control stability differently at different resonant frequencies. Lower resonant frequencies are usually chosen for better filtering performance, which, as shown in the table, makes grid current control unstable. In applications where filter size is crucial, high resonant frequencies are dominant, making the converter current control method more susceptible to instability. However, even if the system is stable due to delays, damping the resonance to improve THD is still desirable. Thus, both control techniques are equivalently susceptible to instability due to the LCL filter resonance depending on values of digital delay and LCL filter resonant frequency, and active damping is needed.

B. ACTIVE DAMPING

The papers [10] and [22] provide a thorough examination of passive and active damping techniques. The most intuitive active damping method is the virtual resistor. The virtual resistor active damping method modifies the controller to simulate the frequency response of the real damping resistor. Based on the findings of the previous papers, a virtual resistor in parallel with the filter capacitor provides excellent damping characteristics while having no effect on lower or higher frequency attenuation. Therefore, this paper focuses on the virtual resistor in parallel with the capacitor technique as seen in Figure 4 using a novel implementation approach for both of the current control methods.

The resistor value can be found in (6), where ζ_d is desired damping ratio of open-loop transfer function in (1) and (2). Active damping can be achieved by modifying the control diagram to simulate a virtual resistor in parallel with the filter capacitor. Figure 5 shows a block diagram of inner current control for both feedback controls, where the red color denotes the parallel virtual connection of the resistor. By using the block diagram modification technique, active damping terms in (4) and (5) can be obtained. As seen from damping transfer functions, both terms contain the same information in numerator $L_{afe}L_gs^2$, while denominator

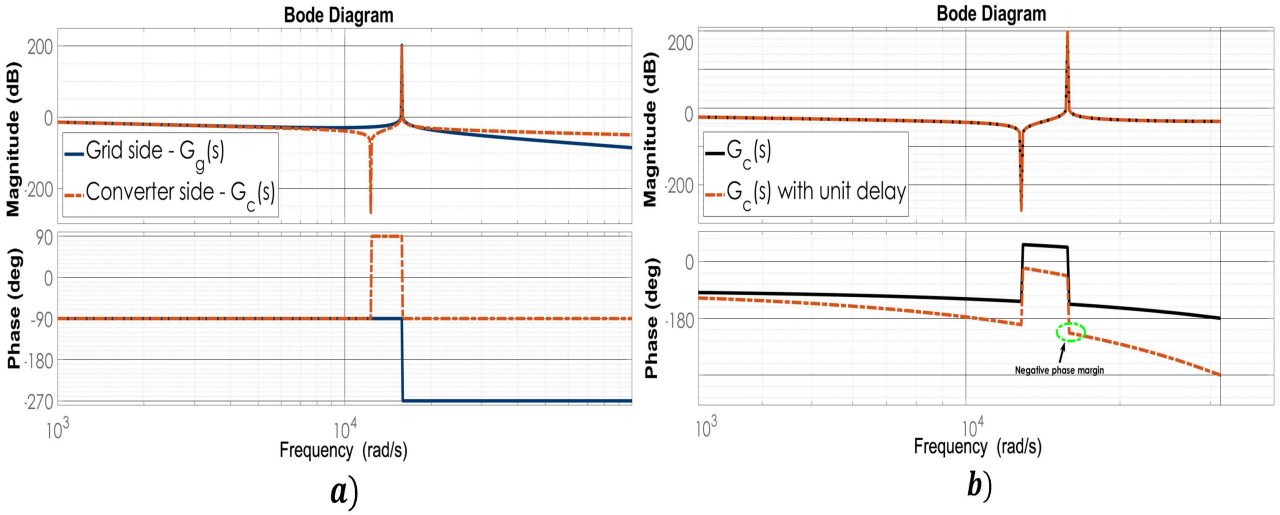

FIGURE 3. a) Open loop grid and converter current control transfer functions. b) Delay effect on converter side current control.

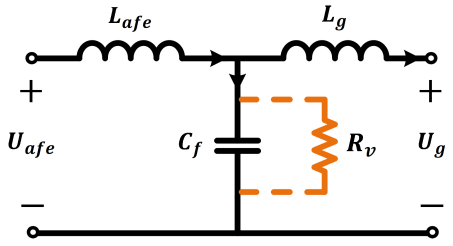

FIGURE 4. Virtual resistor in LCL filter.

consists of virtual resistor R_v gain coupled with additional derivative in converter side feedback control.

$$G_d^g = \frac{L_{afe}L_g s^2}{R_v} \tag{4}$$

$$G_d^c = \frac{L_{afe}L_g s^2}{R_v + R_v L_g C_f s^2} \tag{5}$$

$$R_v = \frac{1}{2\zeta_d \omega_{res} C_f} \tag{6}$$

In fact, when active damping terms are implemented in the feedback loop shown in Figure 5, numerators of (4), (5) become damping poles of the open-loop transfer function mentioned in (1), (2), thus, they contain crucial information needed for implementation of active damping. However, the issue arises for practical implementation of (4), as s^2 term in (4) is not possible to implement due to not being strictly proper transfer function. This paper presents a close approximation of (4) and (5) by keeping the good characteristics as damping of the resonance and negating undesired characteristics of (4) transfer function as a higher gain for frequencies outside of the zone of interest. This way s^2 issue is addressed, and at the same time, damping equivalent for both grid and converter side feedback is developed.

LCL filter is designed based on the trade-off between filter size and current ripple and switching ripple attenuation [23], [24]. In fact, as the resonant frequency decreases in value, the filter's attenuation increases, increasing the physical size of the filter, whereas, for higher values of resonance, the opposite is true. However, stability will also vary depending on the resonant frequency. This has been investigated in [20] where active damping is needed for grid current feedback in low resonant frequency, while not needed in for higher resonant frequency term of stability. In addition to that, grid inductance can also reduce resonant frequency below the critical frequency, making it unstable. Thus, active damping and the control should be stable for a broad range of resonant frequencies.

Many papers have addressed LCL filter resonance damping by analysing two types of current feedback separately, but no universal damping method capable of damping resonance in both cases has been developed. This paper proposes a universal active damping solution that unifies various current control objectives.

C. AFE CONTROL

AFE control is based on voltage-oriented control where the system frame is in a synchronously rotating d-q reference frame. The synchronous rotating frame allows the decoupling of three-phase current into 2-dc components. This way, through controlling I_d, the system is indirectly controlling active power, while through I_q, reactive power can be controlled allowing control of power factor. Desired DC link voltage is accomplished assuming power balance between DC link and AC side. A phase-locked loop is utilized to obtain the phase angle, used in d-q transformation. AFE control seen in simplified control diagram in Figure 6 is represented by following equations Equations (7)–(11).

$$I_d^* = K_{pv}(U_{dc}^* - U_{dc}) + \frac{K_{iv}}{s}(U_{dc}^* - U_{dc}) \tag{7}$$

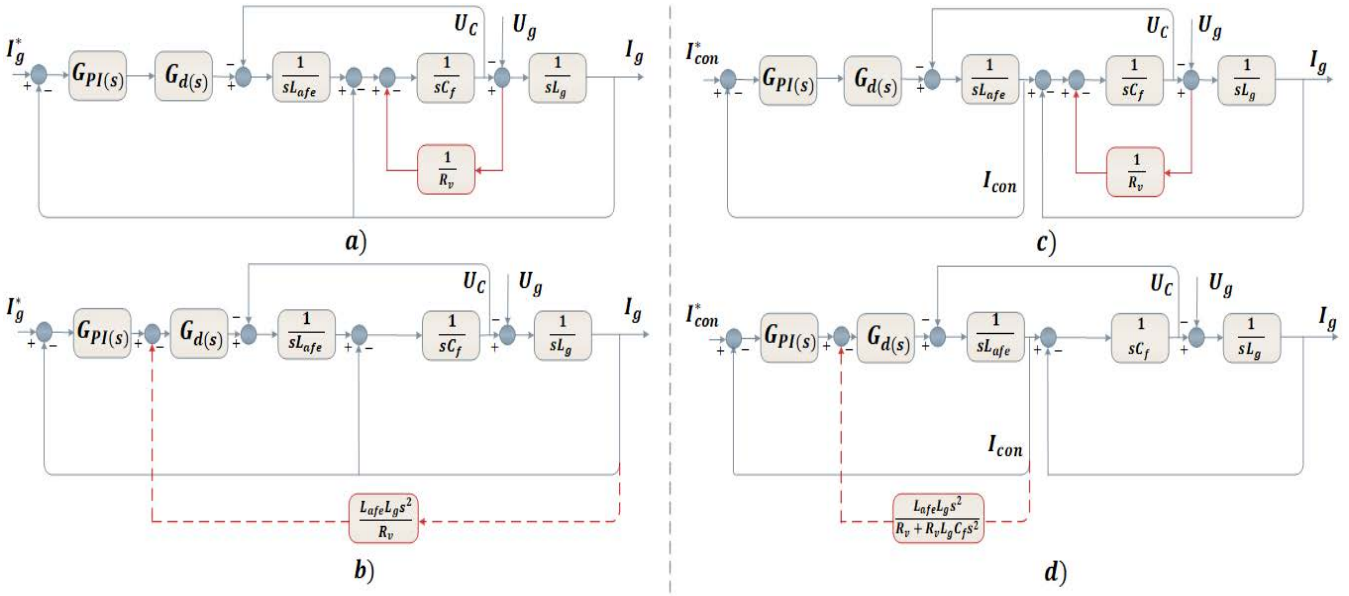

FIGURE 5. a) Grid current control with virtual parallel resistor. b) Grid current control with modified active damping feedback. c) Converter current control with virtual parallel resistor. d) Converter current control with modified active damping feedback.

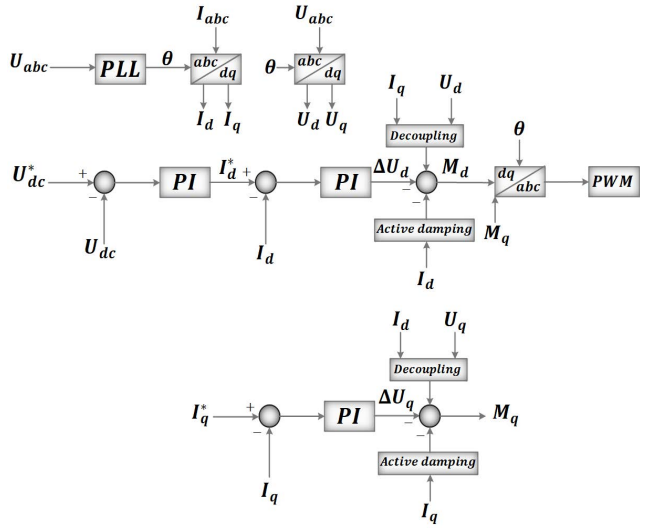

FIGURE 6. Simplified AFE voltage oriented control.

I_q reference is set to 0 in order to achieve unity power factor.

$$M_d = \underbrace{(-\omega_{line}(L_g + L_{afe})I_q}_{\text{Decoupling}} + \underbrace{U_{gd}}_{\text{Feedforward}} - \Delta U_d)\frac{1}{U_{dc}} \quad (8)$$

$$M_q = \underbrace{(\omega_{line}(L_g + L_{afe})I_d}_{\text{Decoupling}} + \underbrace{U_{gq}}_{\text{Feedforward}} - \Delta U_q)\frac{1}{U_{dc}} \quad (9)$$

where ΔUd, ΔUq are:

$$\Delta Ud = K_{pc}(I_d^* - I_d) + \frac{K_{ic}}{s}(I_d^* - I_d) \quad (10)$$

$$\Delta Uq = K_{pc}(I_q^* - I_q) + \frac{K_{ic}}{s}(I_q^* - I_q) \quad (11)$$

where M_d, M_q are modulation indices, while other parameters, later used in simulation and stability analysis are defined in Table 2. To make this controller equivalent for both control methods, in case of the converter feedback, the measured current is multiplied with a gain of -1. Also, for the converter feedback control method, I_q^* quadrature current reference set to $\omega_o C_f U_g$ instead of to 0 as in grid current feedback control. The reason is that grid current is not directly controlled in the converter feedback method.

TABLE 2. Base active front end parameters.

Parameter	Parameters values		
	Notation	Value	Unit
Grid voltage	U_g	220	V(RMS)
Grid frequency	f_g	50	Hz
DC Link voltage	U_{dc}	500	V
Grid side inductor	L_g	2	mH
Converter side inductor	L_{afe}	3.1	mH
Filter capacitor	C_f	3.3	μF
Resonant frequency	f_{res}	≈ 2.5	kHz
Switching frequency	f_{SW}	10	kHz
Sampling frequency	f_s	10, 20	kHz
Virtual resistor	R_v	13.07	Ω
Current PI controller	K_{pc}, K_{ic}	5, 3000	
Voltage PI controller	K_{pv}, K_{iv}	0.02, 3	
Damping knobs active damping	ζ_1, ζ_2	4, 0.707	

Tuning of PI controller parameters can be done using modulus optimum technique for the inner current loop and symmetrical optimum technique for the outer DC voltage loop [25]. Additionally, the PI controller parameters can be optimized through frequency response analysis or through a heuristic approach.

III. PROPOSED ACTIVE DAMPING FILTER

This section proposes a novel **4th** order filter for both feedback control mechanisms and a systematic step-wise design procedure for the practical implementation of grid and converter side current active damping. The primary goal of active damping is to simulate the frequency behaviour of the LCL filter as if it had a resistor in parallel with the filter capacitor. To do so, the s^2 term in (4) has to be implemented correctly so that it keeps all the required characteristics while negating problematic ones. Due to the nature of s^2 and infinite gain at a higher frequency, practical implementation is not achievable as a result of unwanted noise amplification in addition to not being a strictly proper transfer function. Therefore, s^2 needs to be approximated so that approximation replicates low and mid-range frequency responses while also attenuating higher frequencies. Therefore, the damping term is desired to have low magnitude at low and high frequencies, high magnitude at the LCL filter resonant frequency. Different approximation techniques have already been introduced as 1^{st} and 2^{nd} order high pass filter [16], [26], however, 1^{st} order high pass filter does not meet the specification of the same slope as s^2 since it introduces only 20 dB/dec which changes the low-frequency response of the system. The second-order high pass filter satisfies low-frequency response but has flat gain after resonant frequency and does not attenuate high-frequency noise in addition to non intuitive tuning. Thus, as an alternative to G_d as per (4), (5) a new filter is introduced in (12) to solve the mentioned problems.

$$G_{Ad} = \pm\frac{L_g L_{afe}}{R_v}\frac{s^2}{\underbrace{\left(\frac{s^2}{\omega_{res}^2}+\frac{2\zeta_1 s}{\omega_{res}}+1\right)}_{\text{Overdamped pole pairs}}\underbrace{\left(\frac{s^2}{\omega_{res}^2}+\frac{2\zeta_2 s}{\omega_{res}}+1\right)}_{\text{Underdamped pole pairs}}} \tag{12}$$

Active damping term in (12) introduces 2 pairs of overdamped and slightly underdamped poles. Damping coefficients ζ_1 and ζ_2 govern system stability. If both pairs of poles are critically damped, depending on virtual resistor value, the system would not satisfy phase frequency response requirements and would become unstable. However, by overdamping 1 pair of poles, and slightly under damping other pair of poles, the system satisfies phase margin and provides stability. Depending on the current control method used, a plus or minus sign is placed in front of the filter to satisfy either phase lead or phase lag at resonant frequency introduced by LCL resonance. The systematic approach to stabilize the arbitrary system is proposed in the following subsections.

A. STEP WISE DESIGN PROCEDURE

To reproduce damping frequency behavior as there is a resistor in parallel with the filter capacitor, the active damping term from (12) is introduced. The following steps ensure a damped stable system:

1) SELECTION OF THE ω_{res}

According to specification, firstly, ω_{res} in (12) is set to resonant frequency (13) of the LCL filter. This will assure that the active damping term approximately follows $+40\ dB/dec$ until the resonant frequency, after which it drops off by $-40\ dB/dec$.

$$\omega_{res} = \sqrt{\frac{L_g + L_{afe}}{L_g L_{afe} C_f}} \tag{13}$$

By setting ω_{res} to the resonant frequency, active damping will closely satisfy two requirements, accurate magnitude response of s^2 to resonant frequency and noise attenuation after resonant frequency.

2) SELECTION OF THE DAMPING TERMS ζ_1 AND ζ_2

Damping term ζ_2 in (12) is set to 0.707, and ζ_1 is varied. Figure 7 shows the LCL filter grid current feedback open-loop transfer function with implemented active damping and how the system is unstable due to phase-frequency response mismatch if over-damped pair of poles are not damped enough. For comparison purposes, Figure 7 also includes a system with no active damping implemented. As seen in the figure, an increase in damping constant ζ_1 leads to a stable system due to earlier roll-off frequency. However, overdamping can lead to resonance damping degradation as the filter due to earlier roll-off does not follow the active damping term in (4) accurately enough. Therefore, ζ_1 should be selected to be high enough to satisfy phase response characteristics, and low enough so that early roll-off frequency does not deteriorate the damping of the resonance. It is important to note, swooping through different resonant frequencies shows that ζ_1 between 2 and 3 provides the best damping performance and stability margins, however, this is only by ignoring the digital delay effect on stability. In the later section, consideration of digital delay will introduce the additional term to compensate for the digital delay in active damping.

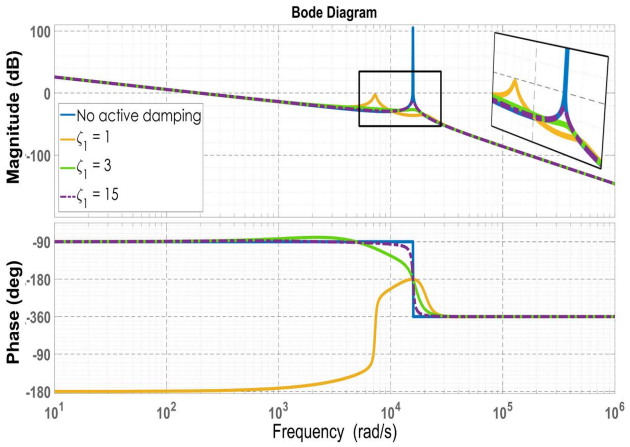

FIGURE 7. Open loop transfer function frequency response with manipulation of ζ_1.

3) SELECTION OF THE VIRTUAL RESISTOR R_V AND PHASE-SHIFTING

As a final step, two unknowns need to be determined to properly implement active damping. The virtual resistor value is calculated based on the equation presented in (6). After determining the virtual resistor value, the active damping sign is left to determine. As mentioned previously, the active damping sign depends on the type of control used. If grid current active damping is used, based on the bode diagram shown in Figure 3, phase lag at resonant frequency needs to be compensated, therefore, a negative sign in front of the active damping is used for grid current control. In the case of converter current control, it will be exactly the opposite, therefore, plus sign is added in front of active damping.

As seen in step by step design procedure, tuning of the active damping is relatively simple and intuitive. As long as LCL filter parameters and ω_{res} are known, good damping performance is achievable as it will be shown in later sections.

B. COMPARISON OF PROPOSED FILTER VS EXISTING METHODS

To highlight the advantages of the proposed active damping control, a comparison with existing methods for grid current feedback control is shown in the following Figure 8. Grid current feedback control method is considered in the low resonant frequency ω_{res} range where the system is least stable. 1st and 2nd order filters are tuned based on the heuristic approach presented in [26]. As shown, proposed active damping offers the best attenuation of the resonant frequency, better harmonic rejection at 150 Hz, a much bigger phase margin, and a better gain margin. The reason for this is that more poles provide a higher degree of freedom, which increases robustness when parameters change. In addition to the advantages seen in the figure, proposed active damping offers more intuitive tuning based on LCL filter resonant frequency compared to existing methods. Proposed active damping also assures stability for the wide range of resonant frequencies. In summary, the main goal of the virtual resistor technique is to simulate resistor in parallel with the filter capacitor, and the proposed filter offers a closer approximation of the passive resistor frequency response.

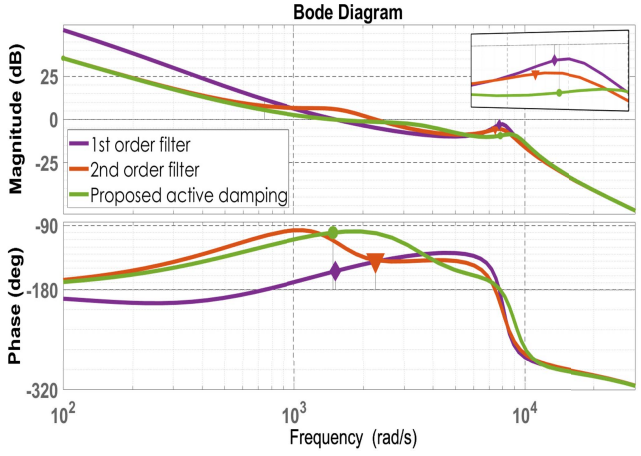

FIGURE 8. Comparison of proposed vs existing damping filters.

C. SENSITIVITY TO SWITCHING AND LOW-ORDER HARMONICS

The impedance of the AFE LCL filter changes when active or passive damping is used. This can make the system more sensitive to specific harmonics, which can be harmful. The optimum damping technique should have no effect on harmonics other than the resonant frequency, which is the frequency of interest. As mentioned previously, this is one of the inherent advantages of using proposed active damping. In Figure 9, the grid current admittance magnitude for the proposed active damping represented in purple color is compared to passive damping with a resistor in series with the capacitor shown in orange color, as well as the worst-case scenario with no damping in green color. For low order and switching harmonics, the proposed active damping has little to no effect on frequency response, as shown in the figure. Passive damping, for example, increases sensitivity to switching harmonics, which can be detrimental to the system. As can be seen from the analysis, active damping only affects the frequency of interest.

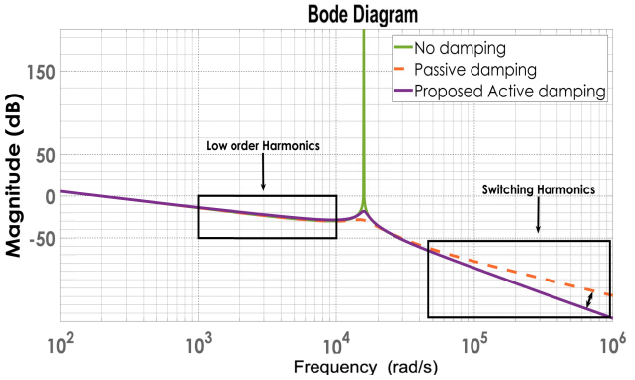

FIGURE 9. Sensitivity to lower order and switching harmonics.

D. DISCRETIZATION OF THE PROPOSED FILTER

As control algorithms are employed on the digital controller, there is a concern with the effect of digital delays. Considering that the current is sampled at the beginning of each switching period, the conversion time of the A/D converter and calculation time of the digital controller will introduce delays in the control loop. Digital delays could weaken system stability margin, and possibly induce system instability [27], [28]. In the previous section, the system has been analyzed considering only for continuous domain, and ignoring the effect of a digital delay. Additional phase delay will, in fact, have an extensive negative effect on system stability depending on LCL filter resonant frequency. Therefore, to analyze system stability, it is necessary to discretize both systems shown in Figure 5 starting from the main contribution

of this paper, proposed active damping. Proposed **4th** order filter from (12) is discretized using Tustin method.

$$G_{Adz} = \pm\frac{a+b}{c\,d} \tag{14}$$

where,
$a = 4\,L_{afe}\,L_g\,T_s^2\,w_{res}^4\,z^4 - 8\,L_{afe}\,L_g\,T_s^2\,w_{res}^4\,z^2$,
$b = 4\,L_{afe}\,L_g\,T_s^2\,w_{res}^4$,
$c = R_v\,(4\,\zeta_2\,T_s\,w_{res}\,(z^2-1) + T_s^2\,w_{res}^2(z+1)^2 + 4\,(z-1)^2)$,
$d = T_s^2\,w_{res}^2\,(z+1)^2 + 4\,T_s\,w_{res}\,(z^2-1)\,\zeta_1 + 4\,(z-1)^2$
Delay G_{dz} is approximated to a z^-1 considering worst-case scenario for computational, PWM and transport delay. However, bearing in mind the digital delay introduced by sampling, computation, and PWM, for specific resonant frequencies, the phase will be shifted into an unstable region, resulting in a frequency response that differs from that of continuous systems in the discrete domain. Thus, to keep with the requirements stated in previous sections, the additional term will be added into active damping to assure stable performance in a wide range of LCL filter resonant frequencies. The term added is a simple zero ($s\,T_s$) in continuous domain adding 90 degrees of phase lead, when discretized becomes the following term:

$$G_{comp} = \frac{2\,z-2}{z+1} \tag{15}$$

For grid and converter current feedback control, both transfer functions (1), (2) are discretized using zero order hold, thus, including sampling delay.

$$G_{gZ} = \frac{T_s}{a(z-1)} - \frac{\sqrt{b}(z-1)\sin\left(T_s\sqrt{\frac{a}{b}}\right)}{a^{3/2}\left(-2z\cos\left(T_s\sqrt{\frac{a}{b}}\right)+z^2+1\right)} \tag{16}$$

$$G_{cZ} = \frac{(z-1)(ac-b)\sin\left(T_s\sqrt{\frac{a}{b}}\right)}{a^{3/2}\sqrt{b}\left(-2z\cos\left(T_s\sqrt{\frac{a}{b}}\right)+z^2+1\right)} + \frac{T_s}{a(z-1)} \tag{17}$$

where, $a = L_g + L_{afe}$, $b = L_g L_{afe} C_f$ and $c = L_g C_f$. Lastly, the PI controller is discretized using the Tustin transformation method in (18).

$$G_{PIz} = K_{pc} + K_{ic}\frac{\mathrm{Ts}(z+1)}{2(z-1)} \tag{18}$$

Combining all discrete transfer function yields system shown in Figure 10. The closed-loop transfer function of the system in the mentioned figure is analyzed for stability in the following section.

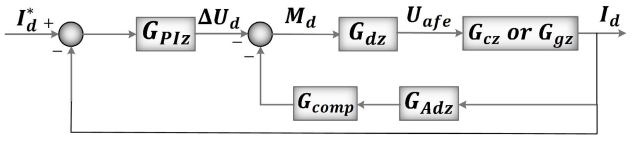

FIGURE 10. Inner current control loop with active damping.

IV. STABILITY ANALYSIS

The main concern with LCL filter resonance is the stability. The magnitude peak at resonance will include phase lag or lead (depending on control method) that drives the system to instability. To compensate for phase lag or lead, active damping is used to dampen the magnitude peak. However, depending on the application, LCL filter and grid impedance can change, which will affect the stability and performance of active damping on current control. As a result, the following section investigates the impact of changes in LCL filter parameters and grid impedance on stability margin under double update PWM sampling.

A. EFFECT OF DIFFERENT RESONANT FREQUENCY ON STABILITY

Active damping that can damp resonance and keep the system in a stable region for a wide range of resonant frequencies is critical. The selection of the resonant frequency depends on a designer and LCL filter, however, resonance can drift from expected values, depending on grid impedance. Thus, active damping should be able to stay stable for a broad spectrum of resonant frequencies.

Figure 11 represents the root loci of the system in Figure 10. Root loci is plotted for 3 different resonant frequencies by changing filter capacitor value. The most prominent conclusion is that proposed active damping assures stability for both control strategies as poles are inside of the unit circle with adequate stability margins. In the case of the grid current control, Figure 11 a), especially for frequencies above 1500 Hz system guarantees sufficient gain and phase margin, and damping performance, however, for the low range of resonant frequencies, poles are moving to the boundaries of the unit circle, resulting in the lower gain margin. As critical frequency for double update PWM for the investigated system is 3.34 kHz, without active damping, the region below critical frequency is unstable.

In the case of the converter current control, Figure 11 b), it is obvious that active damping offers sufficient stability margins. Poles at the highest resonant frequency are closest to becoming unstable, but still with high enough safety margins. As shown in Table 1, a system with that resonant frequency and no active damping is usually unstable. Thus, from the stability point of view, it can be concluded that the proposed active damping helps in damping resonant poles for a wide range of resonant frequencies, therefore, it provides a robust active damping method that is independent of LCL filter parameters.

B. GRID IMPEDANCE EFFECT ON STABILITY

In practical industrial applications, weak grid, grid impedance unpredictability, or LCL-filter degradation can lead to model uncertainty. Specifically, the grid side filter inductor, L_g parameter will be combined with the grid inductance value L_{gpar} which in practical operations cannot be identified. Therefore, it is important that active damping

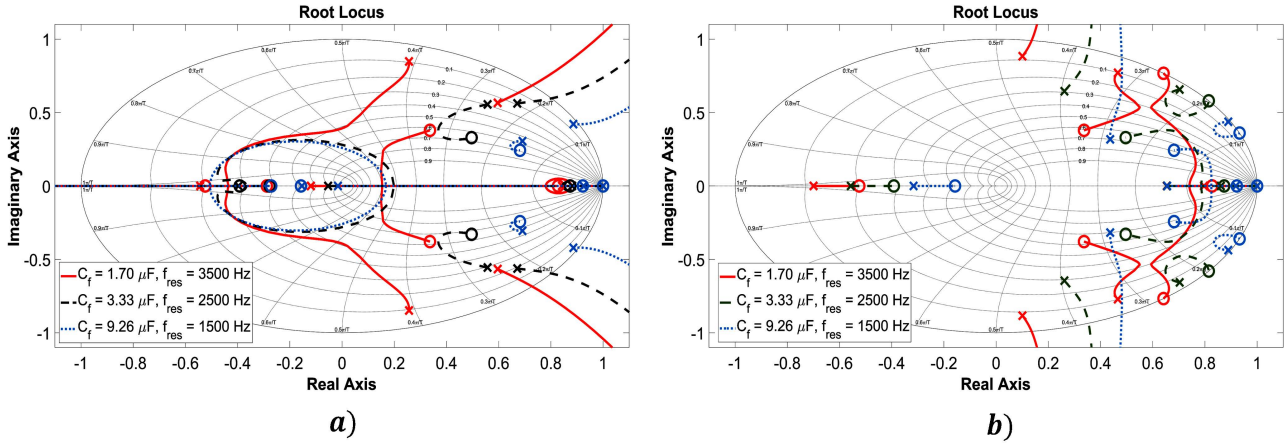

a) *b)*

FIGURE 11. Root loci variation to different resonant frequencies. a) Root loci for grid current control. b) Root loci for converter current control.

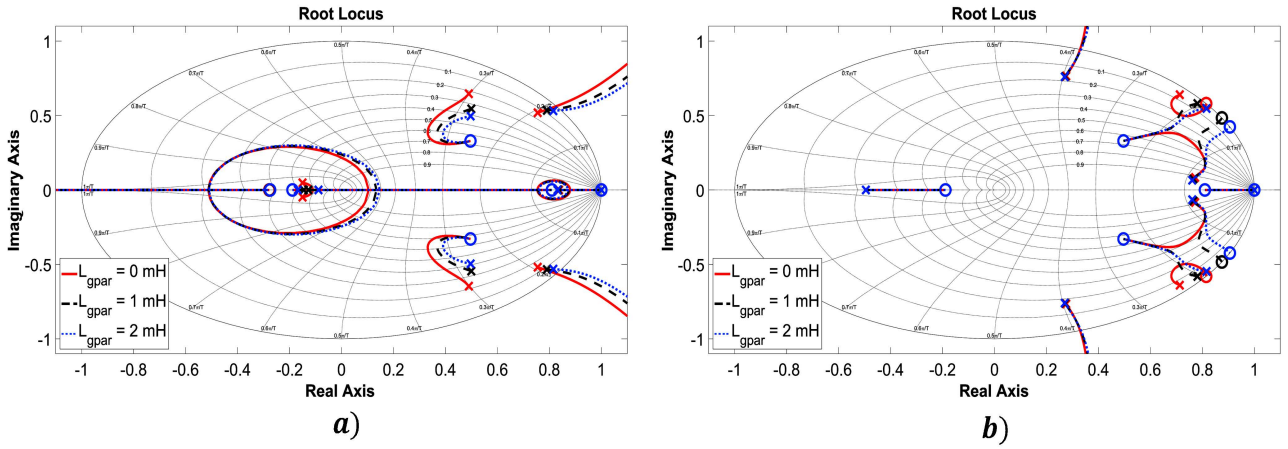

a) *b)*

FIGURE 12. Root loci variation to different grid impedance. a) Root loci for grid current control. b) Root loci for converter current control.

can provide robustness to grid inductor parameter variation. As active damping depends on model accuracy in (12), it is important to investigate the performance of the proposed control considering total L_g uncertainty. Grid impedance effect on stability based on double update PWM and resonant frequency of 2500 Hz can be seen in Figure 12. Figure a) shows grid current control impedance effect on complex resonant poles on the right of the unit circle. As grid inductance is increased, complex poles are moving closer to the unit circle, reducing the stability margin associated with the poles. However, even in the presence of excessive grid impedance, for a reasonable proportional gain, the system remains in the stable region. The grid impedance effect on stability increases as the resonant frequency decreases. However, this is an expected drawback for most of the control well known in power electronics control engineering. Despite these facts, the proposed active damping provides excellent resistance to external effects such as grid impedance.

Figure 12 b) illustrate poles movement for the converter current control due to grid impedance. Grid impedance has no significant effect on stability margins. Thus, from the provided analysis, grid impedance affects stability, however, even under a weak grid, stability can be assured.

V. RESULTS

A. SIMULATION

To evaluate the proposed filter (14), a system in Fig. 6 with parameters values in Table 2 is simulated in MATLAB/Simulink. As the system in Table 2 is inherently unstable, simulations validations verify filter effectiveness of the proposed filter in damping resonant frequency. In the simulation, the effect of delay and sampling is included to replicate real system behavior.

Measured grid current waveforms can be seen in Fig. 13. At the start, the proposed active damping method is connected to the inner current control until 0.49 s, when active damping is disconnected, the system immediately becomes unstable due to resonance until the 0.51 s when active damping is connected again, and resonance is properly damped through modified control. This simulation evaluates stabilizing grid

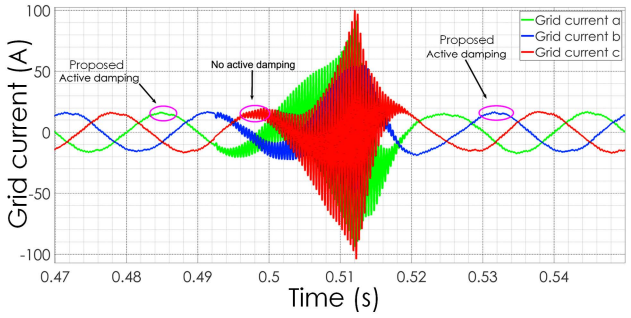

FIGURE 13. Simulation of proposed active damping grid current.

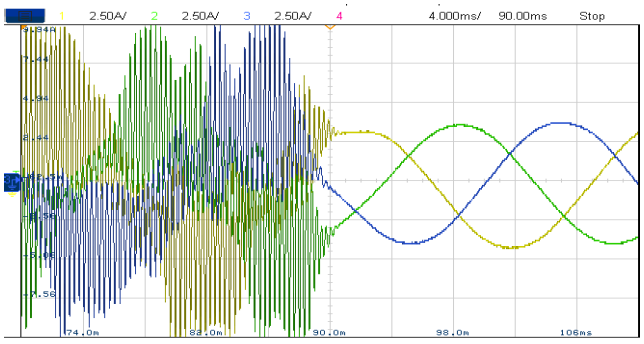

FIGURE 15. Grid current waveforms for the proposed active damping.

current control, however, the same result is obtained when active damping is implemented for converter current control.

B. EXPERIMENTS

To validate the simulations, proposed active damping had to be tested on real hardware. The hardware seen in Figure 14 consists of dSPACE MicroLabBox as a controller, 2 level AFE and inverter boards, LCL filter boards for each phase, required voltage and current sensors, and grid simulator as a voltage source. As shown in the figure, hardware has grid side and converter side current sensors. This way, both controls can be easily implemented.

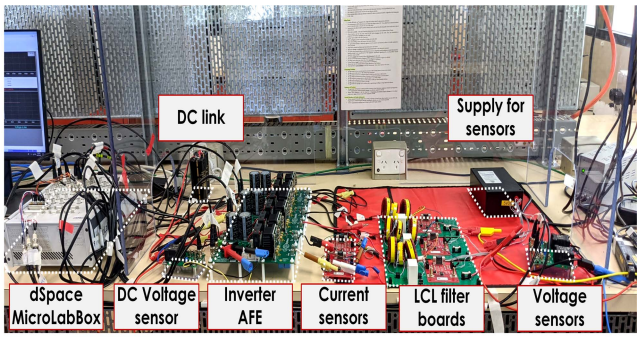

FIGURE 14. Hardware setup.

1) GRID AND CONVERTER CURRENT CONTROL DAMPING PERFORMANCE

Firtsly, the proposed active damping is put to the test in terms of the grid current control method. Due to the LCL filter resonance, lack of passive damping, and double update PWM sampling where the sampling frequency is ($f_s = 2f_{SW}$) system is inherently unstable which is also verified before the implementation of active damping (as shown in Table 1). The reason for system instability is f_{res} which is lower than critical frequency (3) for grid current double update control, therefore, the currents are unstable if no damping is implemented.

Figure 15 depicts measured grid current at 2 different states. At the beginning, active damping is not connected, and only damping is provided by parasitic resistances in the LCL filter, thus, currents are unstable due to high resonance. The proposed active damping is turned on at 90 milliseconds, and the system instantly stabilises, confirming previous simulations. As shown in the figure, the proposed active damping reacts very quickly, providing sufficient damping in a matter of milliseconds. For the converter side current control, similar to grid current control, firstly, the system has to be unstable without active damping. This happens for the same hardware when the sampling frequency is changed to single update sampling ($f_s = f_{SW}$). For a single update, the same value of f_{res} is now above critical frequency, and the system is inherently unstable. However, active damping is more than capable of damping the resonance induced in the current. To avoid repetition, the reader can refer to Figure 15 as the performance is exactly the same.

2) TRANSIENT RESPONSE OF THE PROPOSED ACTIVE DAMPING

The importance of transient response in power electronics cannot be overstated. Different grid conditions can induce transients in the AFE system. Unexpected transients caused by load changes can jeopardise system stability. Particularly in motor drives, where the power flow from the grid is dependent on the varying motor load. Grid voltage abnormalities such as voltage sags and interruptions can also cause transients. When there is a power imbalance between the AC and DC sides due to a short-term grid voltage reduction, the controller adjusts the current reference to keep the DC-link equal to the setpoint reference, resulting in grid current increase and induced transients. Thus, the inherent AFE ability to ride through different grid voltage irregularities is due to the controller's fast reaction to step-change current. Therefore, proposed active damping is investigated under transients.

Figure 16 shows grid current control damped by proposed active damping under transients. As can be seen, at -1.21 milliseconds, the controller increases the current, however, induced transients are properly damped. As a result, the proposed active damping has no negative effects on the control during transients.

As a result, it is clear that the proposed active damping can dampen the resonance induced in both control methods.

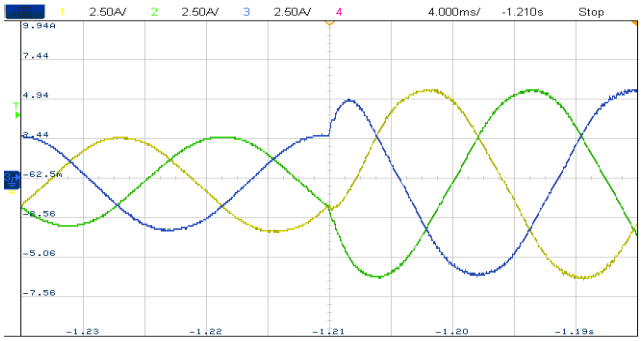

FIGURE 16. Grid current waveforms for the proposed active damping under transients.

VI. CONCLUSION

As the power electronics industry is focusing on economical and robust control solutions, this paper considers an AFE system where sensor number is minimized, and, at the same time, improves the system performance. In the grid current feedback AFE, and the converter current feedback AFE, active damping is implemented using control objective current measurements to remove the LCL filter resonance issue. This paper proposes a novel filter for the practical active damping implementation removing the impracticality of implementing s^2 term derived in equation (4) and presents a unifying approach for two different possible control methods.

A novel filter design procedure is presented to stabilize and damp any arbitrary LCL-filter resonance. As LCL filter parameter choice is up to the designer, it is crucial that active damping can assure the stability for different LCL filter resonant frequencies. This study explores the stability region and displays that proposed active damping is capable of keeping the system stable for a spectrum of different resonant frequencies.

In addition to that, the proposed active damping performance is verified through extensive simulation. Simulations provide a comprehensive analysis of the proposed control and demonstrate satisfying damping characteristics of the novel active damping proposed in this paper. Further, through experimental validation it is shown that both inherently unstable systems can be damped using the proposed active damping filter. Thus, it can be concluded that the proposed active damping can be used in either converter or grid-side current feedback control mechanism and provide good damping performance independent of LCL filter parameters.

REFERENCES

[1] R. T. Jacob and R. Liyanapathirana, "Technical feasibility in reaching renewable energy targets; case study on Australia," in *Proc. 4th Int. Conf. Electr. Energy Syst. (ICEES)*, Feb. 2018, pp. 630–634.

[2] A. Moradi, J. Yaghoobi, A. Alduraibi, F. Zare, D. Kumar, and R. Sharma, "Modelling and prediction of current harmonics generated by power converters in distribution networks," *IET Gener., Transmiss. Distrib.*, vol. 15, no. 15, pp. 2191–2202, Aug. 2021.

[3] D. Kumar and F. Zare, "Harmonic analysis of grid connected power electronic systems in low voltage distribution networks," *IEEE Trans. Emerg. Sel. Topics Power Electron.*, vol. 4, no. 1, pp. 70–79, Mar. 2016.

[4] K. Gharani Khajeh, D. Solatialkaran, F. Zare, and N. Mithulananthan, "Harmonic analysis of grid-connected inverters considering external distortions: Addressing harmonic emissions up to 9 kHz," *IET Power Electron.*, vol. 13, no. 10, pp. 1934–1945, Aug. 2020.

[5] *IEEE Draft Recommended Practices and Requirements for Harmonic Control in Electric Power Systems*, Standard IEEE P519/D6ba, Sep. 2013, pp. 1–26.

[6] T. Sawa and T. Kume, "Motor drive technology–history and visions for the future," in *Proc. IEEE 35th Annu. Power Electron. Spec. Conf.*, Jan. 2004, pp. 2–9.

[7] Y. Mishra, G. Ledwich, A. Ghosh, and T. George, "Long term transmission planning to meet renewable energy targets in Australia," in *Proc. IEEE Power Energy Soc. Gen. Meeting*, Jul. 2012, pp. 1–7.

[8] B. Frieske, M. Kloetzke, and F. Mauser, "Trends in vehicle concept and key technology development for hybrid and battery electric vehicles," in *Proc. World Electric Veh. Symp. Exhib. (EVS27)*, Nov. 2013, pp. 1–12.

[9] J. Xu and S. Xie, "LCL-resonance damping strategies for grid-connected inverters with LCL filters: A comprehensive review," *J. Mod. Power Syst. Clean Energy*, vol. 6, no. 2, pp. 292–305, Mar. 2018. [Online]. Available: https://ieeexplore.ieee.org/abstract/document/9024341, doi: 10.1007/s40565-017-0319-7.

[10] C. Zhang, T. Dragicevic, J. C. Vasquez, and J. Guerrero, "Resonance damping techniques for grid-connected voltage source converters with LCL filters—A review," in *Proc. IEEE Int. Energy Conf.*, May 2014, pp. 169–176.

[11] Y. Lei, W. Xu, C. Mu, Z. Zhao, H. Li, and Z. Li, "New hybrid damping strategy for grid-connected photovoltaic inverter with LCL filter," *IEEE Trans. Appl. Supercond.*, vol. 24, no. 5, Oct. 2014, Art. no. 0601608.

[12] R. Peña-Alzola, M. Liserre, F. Blaabjerg, R. Sebastián, J. Dannehl, and F. W. Fuchs, "Analysis of the passive damping losses in LCL-filter-based grid converters," *IEEE Trans. Power Electron.*, vol. 28, no. 6, pp. 2642–2646, Jun. 2013.

[13] R. N. Beres, X. Wang, F. Blaabjerg, M. Liserre, and C. L. Bak, "Optimal design of high-order passive-damped filters for grid-connected applications," *IEEE Trans. Power Electron.*, vol. 31, no. 4, pp. 2083–2098, Mar. 2016.

[14] Z. Ma, L. Zhou, and J. Liu, "Proportional capacitor current feedback based active damping control for LCL-filter converters with considerable control delay," in *Proc. IEEE Appl. Power Electron. Conf. Expo. (APEC)*, 2020, pp. 3110–3114.

[15] J. Samanes and E. Gubia, "Active damping based on the capacitor voltage positive-feedback for grid-connected power converters with LCL filter," in *Proc. 21st Eur. Conf. Power Electron. Appl.*, 2019, pp. 1–10.

[16] X. Wang, F. Blaabjerg, and P. C. Loh, "Grid-current-feedback active damping for LCL resonance in grid-connected voltage-source converters," *IEEE Trans. Power Electron.*, vol. 31, no. 1, pp. 213–223, Jan. 2016.

[17] D. Pérez-Estévez, J. Doval-Gandoy, A. G. Yepes, S. López, and F. Baneira, "Generalized multifrequency current controller for grid-connected converters with LCL filter," *IEEE Trans. Ind. Appl.*, vol. 54, no. 5, pp. 4537–4553, Oct. 2018.

[18] T. Dragicevic, C. Zheng, J. Rodriguez, and F. Blaabjerg, "Robust quasi-predictive control of *LCL*-filtered grid converters," *IEEE Trans. Power Electron.*, vol. 35, no. 2, pp. 1934–1946, Feb. 2020.

[19] E. Matijevic, R. Sharma, and F. Zare, "A higher-order filter approach to implement grid current based active damping in active front end converters," in *Proc. IEEE Int. Conf. Power Electron., Drives Energy Syst. (PEDES)*, Dec. 2020, pp. 1–6.

[20] S. G. Parker, B. P. McGrath, and D. G. Holmes, "Regions of active damping control for LCL filters," *IEEE Trans. Ind. Appl.*, vol. 50, no. 1, pp. 424–432, Jan./Feb. 2014.

[21] J. Ma, X. Wang, F. Blaabjerg, L. Harnefors, and W. Song, "Accuracy analysis of the zero-order hold model for digital pulse width modulation," *IEEE Trans. Power Electron.*, vol. 33, no. 12, pp. 10826–10834, Dec. 2018.

[22] C. C. Gomes, A. F. Cupertino, and H. A. Pereira, "Damping techniques for grid-connected voltage source converters based on LCL filter: An overview," *Renew. Sustain. Energy Rev.*, vol. 81, pp. 116–135, Jan. 2018.

[23] A. Reznik, M. G. Simáes, A. Al-Durra, and S. M. Muyeen, "LCL filter design and performance analysis for grid-interconnected systems," *IEEE Trans. Ind. Appl.*, vol. 50, no. 2, pp. 1225–1232, 2014.

[24] D. Solatialkaran, K. G. Khajeh, and F. Zare, "A novel filter design method for grid-tied inverters," *IEEE Trans. Power Electron.*, vol. 36, no. 5, pp. 5473–5485, May 2021.

[25] S. D'Arco, J. A. Suul, and O. B. Fosso, "Automatic tuning of cascaded controllers for power converters using eigenvalue parametric sensitivities," *IEEE Trans. Ind. Appl.*, vol. 51, no. 2, pp. 1743–1753, Mar./Apr. 2015.
[26] J. Xu, S. Xie, and T. Tang, "Active damping-based control for grid-connected LCL-filtered inverter with injected grid current feedback only," *IEEE Trans. Ind. Electron.*, vol. 61, no. 9, pp. 4746–4758, May 2014.
[27] C. Zou, B. Liu, S. Duan, and R. Li, "Influence of delay on system stability and delay optimization of grid-connected inverters with LCL filter," *IEEE Trans. Ind. Informat.*, vol. 10, no. 3, pp. 1775–1784, Aug. 2014.
[28] R. Sharma, F. Zare, D. NesIc, and A. Ghosh, "A hidden block in a grid connected active front end system: Modelling, control and stability analysis," *IEEE Access*, vol. 5, pp. 11852–11866, 2017.

EDI MATIJEVIC (Member, IEEE) received the M.Sc. degree in energy engineering with specialization in power electronics and drives engineering from Aalborg University, Aalborg, Denmark, in 2019. He is currently pursuing the Ph.D. degree in electrical engineering with The University of Queensland, Brisbane, QLD, Australia. His research interests include power electronics converters design and control, power quality, and electrical drives.

RAHUL SHARMA (Senior Member, IEEE) a Senior Lecturer with the School of Information Technology and Electrical Engineering, The University of Queensland, Australia. His research interests include control of grid connected inverters, demand management algorithms, and monitoring of large solar farms.

FIRUZ ZARE (Fellow, IEEE) received the Ph.D. degree in power electronics from the Queensland University of Technology, Australia, in 2002. He has over 20 years of experience in academia, industry, and international standardization committees, including eight years in two large research and development centers working on power electronics and power quality projects. He is a Professor of power electronics and the Head of the School of Electrical Engineering and Robotics, Queensland University of Technology, Australia. He has published four books, over 280 journal and conference papers, five patents and over 40 technical reports. His main research interests include power electronics topology, control and applications, power quality and regulations, and pulsed power applications. He has received several awards, such as the Australian Future Fellowship, the John Madsen Medal, the Symposium Fellowship, and the Early Career Excellence Research Award. He is a Task Force Leader (International Project Manager) of the Active Infeed Converters to develop the first international standard IEC 61000-3-16 within the IEC standardization SC77A. He is a Senior Editor of IEEE Access Journal, a Guest Editor and an Associate Editor of the IEEE Journal of Emerging and Selected Topics in Power Electronics, and *IET Journal*. He is the Editorial Board Member of several international journals.

DINESH KUMAR (Senior Member, IEEE) received the M. Tech. degree in power system engineering from IIT Roorkee, India, in 2004, and the Ph.D. degree in power electronics from the University of Nottingham, U.K., in 2010. From 2004 to 2005, he was a Lecturer at the Electrical Engineering Department, National Institute of Technology, Kurukshetra, India. In 2006, he joined as a Research Fellow of power electronics at Technical University Chemnitz, Germany. Since 2011, he has been with Danfoss Drives A/S, Denmark, where he is involved in many research and industrial projects. He is an Adjunct Associate Professor with the Faculty of Engineering, School of Electrical Engineering and Robotics, Queensland University of Technology, Australia. His current research interests include motor drive, harmonic analysis and mitigation techniques, power quality, and electromagnetic interference in power electronics. He is a member of the IEC Standardization Working Group in TC77A, TC22/SC22G, and SyC LVDC Committee. He was a recipient of two IEEE Best Paper Awards. He is the Editor-in-Chief of *International Journal of Power Electronics* and an Associate Editor of IEEE Transactions on Industry Applications, IEEE Access Journal, and a Member of Editorial Board of *IEEE Transportation Electrification eNewsletter*.